Transmission electron microscopy study of platinum clusters on Al_2O_3/NiAl(110) under the influence of electron irradiation

S. A. Nepijko, M. Klimenkov, H. Kuhlenbeck,[a] and H.-J. Freund
Fritz-Haber-Institut der Max-Planck-Gesellschaft, Abteilung Chemische Physik, Faradayweg 4-6, D-14195 Berlin, Germany

(Received 5 March 1998; accepted 4 December 1998)

Using transmission electron microscopy we have studied the influence of the electron beam in an electron microscope onto platinum clusters deposited on a thin single crystalline γ-Al_2O_3 film grown by oxidation of NiAl(110). At electron current densities below $j \approx 1$ A/cm^2 no influence is observed. Movement and coalescence of clusters occur at electron beam current densities between $j = 2$ and some 10 A/cm^2. For current densities around $j = 50$ A/cm^2 decoration of steps takes place. Further increase to $j = 100$ A/cm^2 and above induces drilling of holes into the substrate by clusters. At such current densities also melting of the clusters may occur. Due to the heat capacity of the system the result does not only depend on the electron current density but also on the irradiation time. © *1999 American Vacuum Society.* [S0734-2101(99)04202-5]

I. INTRODUCTION

Transmission electron microscopy (TEM) is well suited to study deposited clusters. Information on the lattice structure and the morphology as well as on aspects of the chemical composition[1–3] may be obtained. In a previous TEM study[4] and investigations performed under ultrahigh vacuum (UHV) conditions using electron spectroscopy and structural methods[5–10] we have characterized metal clusters deposited on a thin ordered aluminum oxide film grown on NiAl(110) and the oxide film itself with respect to structure and electronic properties. It was shown that small clusters exhibit reduced lattice constants and that their chemical activity differs from that of massive material.[4,7–10] These results are interesting from the viewpoint of catalysis. With TEM single clusters may be studied so that it was possible to establish cluster size/lattice constant relationships. In connection with investigations using infrared spectroscopy, thermal desorption spectroscopy (TDS), and photoelectron spectroscopy [angle resolved ultraviolet photoelectron spectroscopy (ARUPS), x-ray photoelectron spectroscopy (XPS)][7–11] this permitted to trace the chemical activity of the clusters back to structural and electronic properties.

In this publication we will deal with limitations of studies using transmission electron microscopy, i.e., with the influence of the electron beam onto the system. It is known that the electron beam may modify the system. This includes chemical modifications, desorption, and hole formation.[12,13] Clusters on the surface may start to move around and their structure or their shape may change.[14–16] Also charging, coulomb explosion and quasimelting have been reported.[16–20] In order to judge the effect of the electron beam in TEM on the previously studied Pt/γ-Al_2O_3/NiAl(110) system[4] we have exposed this system to electron beams with different current densities. At current densities typically used for TEM no modifications could be observed. However, higher densities led to cluster movement, step decoration, coalescence and, at very high current densities, to burning of holes into the substrate. The latter may in principle be viewed as a method to prepare nanoholes of a well defined diameter.

II. EXPERIMENT

The NiAl(110) sample was circularly shaped with a diameter of about 3 mm and a thickness of approximately 300 μm. It was cut from a NiAl single crystal rod, oriented with Laue backscattering and polished using standard procedures. After this it was bombarded with argon ions ($\approx$3 mA, 5 keV) in an ion milling system (type RES100, made by Baltec) until a small hole with a diameter of about 1 mm was formed in the center of the sample as shown in Fig. 1. In the vicinity of the wedge the sample was sufficiently thin for transmission electron microscopy.

The sample was prepared in an UHV chamber equipped with facilities for ion bombardment and low energy electron diffraction (LEED). In this chamber also the metal clusters were deposited. The oxide film was prepared by oxidation of the NiAl(110) sample at elevated temperature according to a procedure published elsewhere.[21] It is about 5 Å thick and well ordered. Although the oxide exhibits a complicated LEED pattern indicative of a large unit cell in real space its base structure is similar to that of γ-Al_2O_3(111).[21,22] In the vicinity of the wedge also unsupported aluminum oxide is formed so that differences between supported and unsupported oxide could be studied.[23]

Platinum clusters were deposited onto the film by thermal evaporation. The flux of the evaporator was calibrated using a quartz microbalance and the amount of deposited platinum was determined by multiplying the flux by the deposition time.

After oxide preparation and cluster deposition the sample was transferred into the electron microscope. During the transfer the sample was exposed to air for some minutes. It has been shown previously that neither the oxide nor the

[a]Author to whom correspondence should be addressed; electronic mail: Kuhlenbeck@FHI-Berlin.MPG.DE

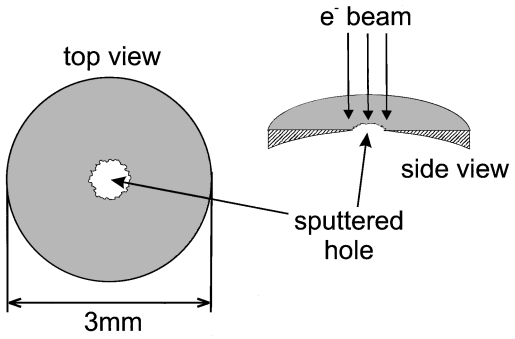

FIG. 1. Schematic drawing of the sample used for the TEM experiments.

clusters are notably modified by this procedure.[23] In particular, the clusters do not get oxidized.

The TEM studies have been performed in a Hitachi 8100 electron microscope with a beam energy of $E_{kin}=200$ keV, beam currents of up to 5 μA (LaB_6 cathode), and an ultimate lattice resolution of 1.44 Å. For spectroscopy means it is equipped with facilities for energy dispersive x-ray analysis (EDX).

Since the studies discussed in this article deal with the influence of the electron beam we had to vary the current density which was achieved by changing the focus of the electron beam and the size of the condenser aperture. For very high electron currents a limiting aperture in beam formation unit was removed.

The experiments were performed as follows: First a high resolution TEM image of the regime chosen for investigation was taken. For this purpose electron current densities of about $j=0.1$ to 2 A/cm^2 were employed which do not lead to visible modifications of the sample according to our studies. After this the sample was irradiated for a defined time with an electron beam of defined intensity. For these experiments the microscope was driven in a mode not suitable for high resolution so that it was not possible to monitor the induced changes by taking TEM images during the irradiation. Therefore a TEM image was taken after the irradiation to document changes in the system. Typically 1–3 min were needed to the change the operation mode of the microscope. Sometimes also several successive cycles of electron beam irradiation followed by recording of a TEM image were employed.

III. RESULTS AND DISCUSSION

In Fig. 2 the effect of electron bombardment with $j=15$ A/cm^2 for 20 s is shown. Irradiation times smaller than 15 s did not induce visible changes, indicating that the effects induced by the electron beam are at least partly of thermal nature. Figure 2(a) has been taken near to the edge of the hole in the sample so that regions with supported (dark region) and unsupported (light region) oxide show up. The small dark spots with diameters of about 10–20 Å are the deposited platinum clusters. Three enlarged parts of Fig. 2(a) are shown in Figs. 2(b) (supported oxide), 2(c) and 2(d) (unsupported oxide). Images of the same regions after electron

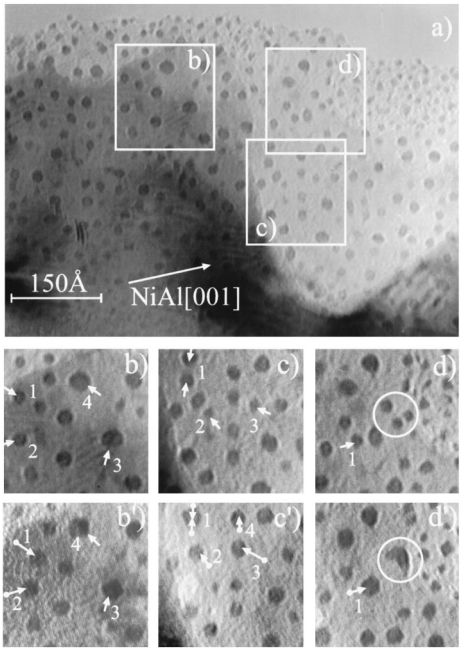

FIG. 2. Structural modifications and motion of Pt clusters due to electron beam irradiation. a) overview taken before irradiation. (b), (c) and (d) different parts of (a). (b′), (c′) and (d′) same regions on the surface as (b), (c) and (d) but after electron irradiation with $j=15$ A/cm^2 ($E_{kin}=200$ keV) for $t=20$ s. The average thickness of the platinum film was one monolayer ($\Theta_{Pt}=1.0$ ML) and the surface temperature during metal deposition was 300 K.

irradiation are displayed in Figs. 2(b′), 2(c′), and 2(d′) so that the irradiation induced modifications are obvious from a comparison with Figs. 2(a), 2(b), and 2(c).

The main effects are motion of clusters and coalescence. No degradation of the oxide film could be detected by visual inspection of the images. Arrows in Figs. 2(a), 2(b), and 2(c) mark clusters that are subject to changes whereas the arrows in Figs. 2(a′), 2(b′), and 2(c′) indicate the directions of cluster movement. There is only one example of cluster movement [e.g., cluster 4 in Figs. 2(c)/2(c′)], but several examples are indicative of coalescence [e.g. 1, 2 in Figs. 2(b)/2(b′), 1, 2, 3 in Figs. 2(c)/2(c′), 1 and the three clusters in the marked regime in Figs. 2(d)/2(d′)]. The marked range in Fig. 2(d′) contains three clusters that are just about to coalesce. As indicated by the complicated shapes of the cluster in 2(d′) the process was possibly not finished when the electron beam was switched off. Of course, also defects on the substrate may lead to the observed shape.

The analysis reveals no obvious differences between clusters on supported and on unsupported oxide. As expected there is a dependency of cluster movement on the cluster size. This is illustrated by the data exhibited in Fig. 2 which show that small clusters with sizes of 10–15 nm are more likely to move than the larger ones. Although movement is unlikely for large clusters there may be changes of the cluster shape towards energetically more favorable ones as indicated by the behavior of clusters 3 and 4 in Figs. 2(b) and 2(b′). Figure 2 shows that the mean diffusion length of the clusters is about 15 Å under the chosen experimental conditions.

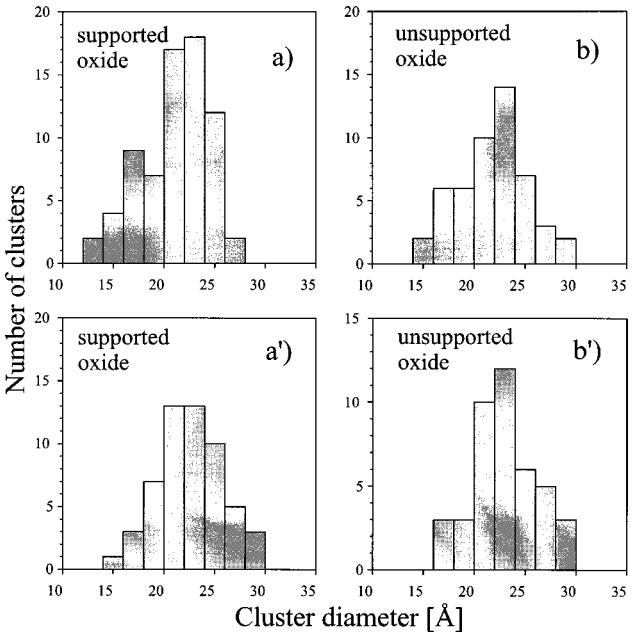

FIG. 3. Pt-cluster size distributions before [(a), (b)] and after [(a′), (b′)] irradiation with a strong electron beam ($j=15$ A/cm^2, $E_{kin}=200$ keV, $t=20$ s). (a) and (a′) are distributions of Pt clusters on supported Al_2O_3 whereas (b) and (b′) correspond to clusters on unsupported oxide. The average thickness of the platinum film was one monolayer ($\Theta_{Pt}=1.0$ ML) and the surface temperature during metal deposition was 300 K.

In Ref. 24 results of studies of platinum clusters on a carbon substrate are reported. On this substrate coalescence of clusters towards multiply twinned particles (MTP) has been observed which may be traced back to the weaker platinum/carbon interaction as compared to the present case where the interaction is strong.[7–11,25]

One interesting point to note is that there is only one observation of cluster movement in Fig. 2 although there are many events of cluster coalescence. If the motion of the clusters on the surface was fully statistical then the motion/coalescence ratio should be different. This indicates that there is some type of far-reaching attractive force between the clusters which is most likely due to a modification of the oxide in the regime near to the clusters. Here modifications of electronic as well as geometric nature have to be considered. This is supported by LEED patterns of $Pt/Al_2O_3/NiAl(110)$ which exhibit strongly damped oxide spots after deposition of only a small amount of platinum.[25]

Since part of the clusters on the surface coalesce under electron beam irradiation there must be a change of the cluster size distribution. This effect is depicted in Fig. 3 where size distributions of clusters on supported [Figs. 3(a)/3(a′)] and unsupported oxide [Figs. 3(b)/3(b′)] are exhibited before and after electron beam irradiation with $j=15$ A/cm^2 ($E_{kin}=200$ keV) for 20 s. The corresponding statistical data are given in Table I. These data show that the cluster density on the surface is reduced by 27% for the unsupported oxide whereas the reduction for clusters on supported oxide is 21%. This is accompanied by an increase of the mean cluster size (see Table I). There are no statistically significant differences between clusters on supported and unsupported oxide.

TABLE I. Statistical data for the distribution of clusters in Fig. 2.

	Unsupported oxide		Supported oxide	
	Before irradiation	After irradiation	Before irradiation	After irradiation
Cluster density [10^{12}/cm^2]	8.4	6.1	7.4	5.8
Covered surface area [%]	20.2	19.4	19.2	18.5
Mean cluster diameter [Å]	19.3	21.4	20.1	22.8
Number of evaluated clusters	72	53	52	41

The effect of different current densities is illustrated in Fig. 4 which shows the evolution of the system after successive irradiation with increasing electron current densities. From visual inspection it is obvious that the cluster size increases with increasing current density. But there is also an effect on the oxide. After irradiation with $j=80$ A/cm^2 the oxide/vacuum borderline appears to be smoothed which points towards melting or other electron beam induced damage of the oxide in this region. This may be the reason for the observation that there are also no clusters near to the borderline in Fig. 4(d). The unsupported oxide near to the NiAl substrate did possibly not melt due to a more efficient transfer of heat into the metal.

Cluster size distributions obtained after irradiation with electron beams of the same current densities as used for the data shown in Fig. 4 are displayed in Fig. 5. This figure clearly supports the conclusion derived from visual inspection of Fig. 4: the mean cluster size increases significantly

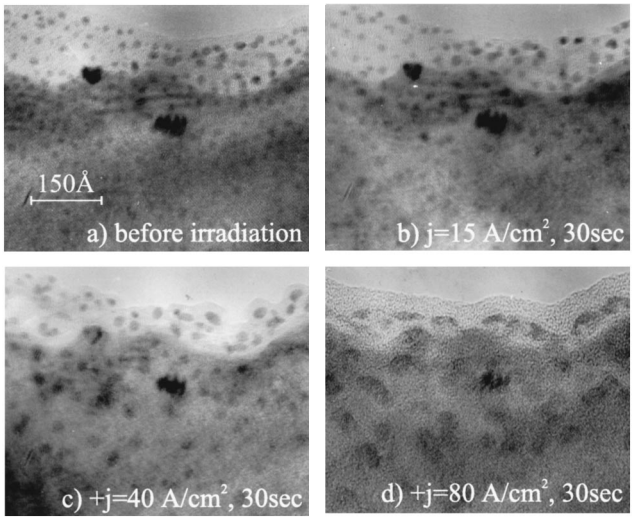

FIG. 4. TEM images of Pt clusters on Al_2O_3/NiAl(110) near to the edge of the wedge obtained after irradiation with electron beams of different intensities ($E_{kin}=200$ keV). (a) before irradiation. (b) $j=10$ A/cm^2, $t=30$ s. (c) additional irradiation with $j=40$ A/cm^2, $t=30$ s. (d) additional irradiation with $j=80$ A/cm^2, $t=30$ s. The average thickness of the platinum film was one monolayer ($\Theta_{Pt}=1.0$ ML) and the surface temperature during metal deposition was 300 K.

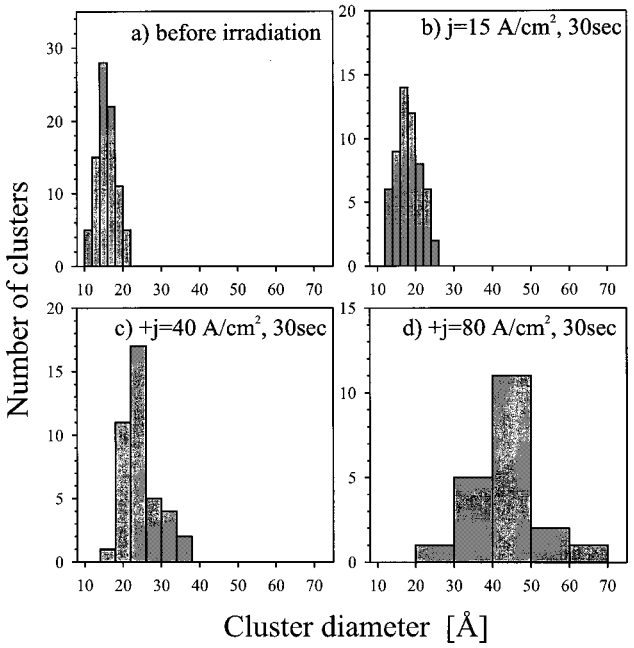

FIG. 5. Pt-cluster size distributions obtained after irradiation of the sample with electron beams of different intensities. (a), (b), (c), and (d) correspond to the four TEM images in Fig. 4. The results shown here include data for clusters on supported and unsupported oxide.

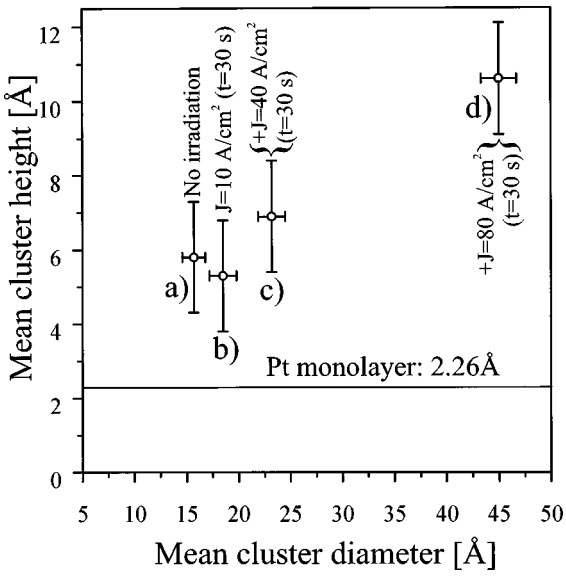

FIG. 6. Average heights of Pt clusters on Al_2O_3/NiAl(110) after irradiation with electron beams with different intensities. These data have been obtained from the results presented in Fig. 5. For the calculation of the heights a cylindrical cluster shape has been assumed. (a), (b), (c), and (d) correspond to the four TEM images displayed in Fig. 4.

with increasing current density. Some statistical data are listed in Table II.

From the statistical data shown in Fig. 5 and the known amount of deposited platinum the mean height of the clusters may be calculated. Results are displayed in Fig. 6. The figure shows that the mean cluster height increases only slightly with increasing mean cluster diameter indicating that the interaction with the oxide is so strongly bonding that the clusters are not able to reduce their surface area by increasing their heights which would minimize the surface free energy. Since the surface areas of the clusters and the direct cluster/oxide interaction energies are approximately the sums of the corresponding values of the clusters before coalescence in the case of rather flat clusters, there may only be a small energy gain upon coalescence when only these energies are considered. However, energies connected with the size of the borders decrease strongly when the clusters coalesce. Here the energies due to the modification of the oxide near to the clusters and the cluster/oxide interaction at the border of the clusters are to be mentioned. Therefore the reduction of these energies may be the main driving force for cluster coalescence.

Current densities above $j = 80$ A/cm^2 lead to decoration of steps on the supported oxide by clusters. This effect is reversible since the decoration is not observed after the electron beam has been switched off. It could not be photographed because the microscope was driven under conditions which prevented image photography so that no image is shown here. Electron diffraction images indicate that the orientation of the clusters with respect to the substrate does not change upon coalescence. As shown previously[1] the orientation of the clusters is Pt[111]‖NiAl[110] and Pt[110]‖NiAl[001].

A further strong increase of the electron current density to values of $j = 150$ A/cm^2 and above leads to an interesting effect. At such current densities the clusters burn holes into the substrate. Hollows as well as deep holes may be formed. Two examples are shown in Figs. 7 and 8. The current densities have been $j = 150$ and 200 A/cm^2, respectively. The structure of the NiAl(110) substrate is still visible at the bottom of some holes showing that these holes do not extend to the bottom of the NiAl wedge. However, platinum clusters were not observed in any of these holes which could be due to insufficient contrast or to formation of an alloy with the NiAl.

TABLE II. Statistical data for the distribution of clusters in Fig. 4.

	No irradiation	15 A/cm^2 30 s	+40 A/cm^2 30 s	+80 A/cm^2 30 s
Cluster density [10^{12}/cm^2]	8.8	6.9	3.1	0.7
Covered surface area [%]	17.3	17.9	14.7	10.3
Mean cluster diameter [Å]	15.8	18.2	24.6	43.5
Number of evaluated clusters	86	57	40	20

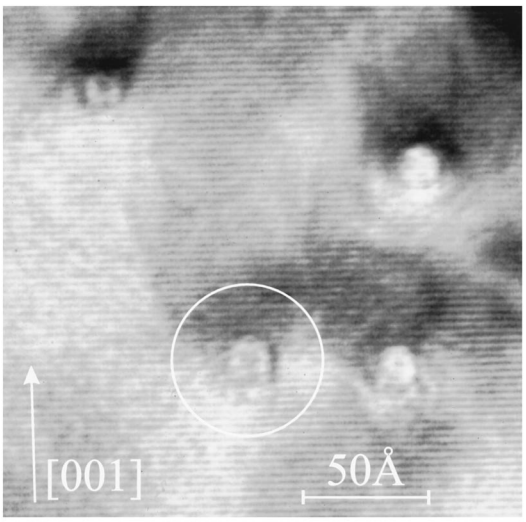

FIG. 7. TEM image obtained after irradiating Pt clusters on Al_2O_3/NiAl(110) with a very intense electron beam ($j=150$ A/cm^2) for 60 s. This image has been taken using only the NiAl[$1\bar{1}0$] beam. The average thickness of the platinum film was one monolayer ($\Theta_{Pt}=1.0$ ML) and the surface temperature during metal deposition was 300 K.

The images displayed in Figs. 7 and 8 have been taken using only the NiAl[$1\bar{1}0$] beam. Therefore the depth Λ of the holes may be calculated according to

$$\Lambda = \frac{n}{\Delta\Theta_{1\bar{1}0}\cdot|\mathbf{g}_{1\bar{1}0}|\cdot\sqrt{1+\dfrac{1}{\xi_g^2\cdot(\Delta\Theta_{1\bar{1}0})^2\cdot|\mathbf{g}_{1\bar{1}0}|^2}}} \tag{1}$$

$$= \underbrace{\frac{n}{\Delta\Theta_{1\bar{1}0}\cdot|\mathbf{g}_{1\bar{1}0}|}}_{\text{(kinematical result)}} \cdot \underbrace{\frac{1}{\sqrt{1+\dfrac{1}{\xi_g^2\cdot(\Delta\Theta_{1\bar{1}0})^2\cdot|\mathbf{g}_{1\bar{1}0}|^2}}}}_{\text{(dynamical correction factor)}}. \tag{2}$$

For details see Ref. 26. The first part of the right side of Eq. (2) is the result of kinematical theory which is corrected for dynamical effects by the second part. $\Delta\Theta_{1\bar{1}0}$ is the tilt angle out of the Bragg condition. Since the electron beam was incident along the [110] direction, this angle is equal to the Bragg angle $\Theta_{1\bar{1}0}$:

$$\Delta\Theta_{1\bar{1}0}=\Theta_{1\bar{1}0}=\frac{|\mathbf{g}_{1\bar{1}0}|}{2|\mathbf{k}_{\text{electron beam}}|} = 6.12\times10^{-3} \text{ in the present case.} \tag{3}$$

$\mathbf{g}_{1\bar{1}0}$ is the $1\bar{1}0$ reciprocal lattice vector of NiAl ($|\mathbf{g}_{1\bar{1}0}|=0.492$ Å^{-1}), ξ_g the extinction distance and n the number of observed extinction fringes. A lower limit for the extinction distance of the NiAl[110] reflex may be estimated from the extinction distance of the 111 reflex of Ni given in Ref. 27 for an energy of 100 keV. At this energy the value is $\xi_g=26.8$ nm which is most likely smaller than the corresponding value at 200 keV. The number given for Ni may be taken since the electron densities in NiAl and Ni are not too different and the 111 reflex has been chosen since for this reflex the extinction length is smallest. With the given value for ξ_g the value of the dynamical correction factor in Eq. (2) is 0.63. This number has to be considered as a lower limit since with increasing extinction length this value increases until it finally reaches a value of 1. For the models of the holes presented in the following we note that the error introduced by the data evaluation is most likely larger than the one introduced be the dynamical correction factor.

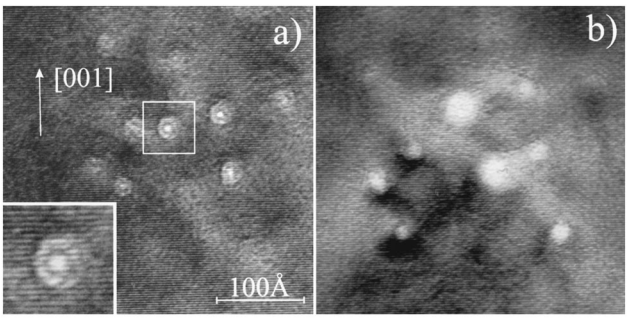

FIG. 8. TEM images obtained after irradiating Pt clusters on Al_2O_3/NiAl(110) with very intense electron beams. (a) $j=200$ A/cm^2, $E_{kin}=200$ keV, $t=40$ s. (b) additional irradiation with the same parameters as in (a). These images have been taken using only the NiAl[$1\bar{1}0$] diffracted electron beam. The average thickness of the platinum film was one monolayer ($\Theta_{Pt}=1.0$ ML) and the surface temperature during metal deposition was 300 K.

The hole marked in Fig. 7 is schematically drawn in Fig. 9(a). It has the shape of a quadratic pyramid with an edge length of 27 Å at the top and an estimated depth of 320 Å. The surface orientations of the side walls are near to $(00\bar{1})$

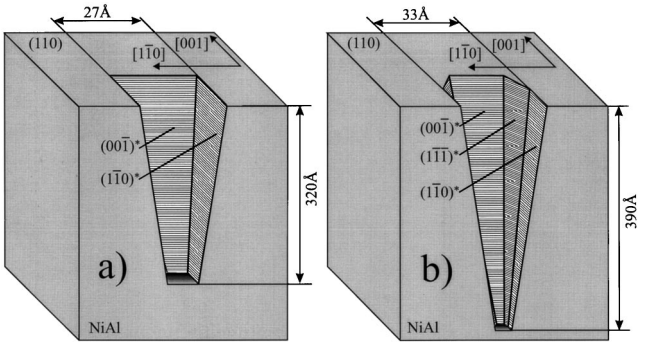

FIG. 9. Models of two types of holes in Al_2O_3/NiAl(110) obtained after irradiation of Pt clusters on the oxide film with very intense electron beams. (a) shape of the hole marked in Fig. 7. (b) shape of the hole marked in Fig. 8. The average thickness of the platinum film was one monolayer ($\Theta_{Pt}=1.0$ ML) and the surface temperature during metal deposition was 300 K.

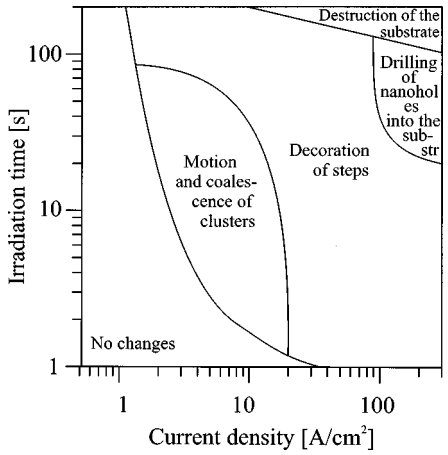

FIG. 10. Estimate of a ''phase diagram'' for the behavior of Pt clusters on Al_2O_3/NiAl(110) as a function of the electron beam density and the irradiation time.

Èand $(1\bar{1}0)$. ''Near to'' means that this would be the case if the walls of the hole were oriented perpendicularly to the surface plane. However, there is a small deviation of about 5° so that the given orientations are only approximate. The orientation which is denoted as $(1\bar{1}0)$* in Fig. 9(a) could, for instance, in reality be $(7\bar{6}0)$, $(8\bar{7}0)$, or $(9\bar{8}0)$. Surface with these orientations display large terraces with $(1\bar{1}0)$ orientation.

Irradiation with $j=200$ A/cm^2 for 40 s leads to even deeper holes [see Fig. 8(a)]. Also the shapes of the holes are different; they are not quadratic as the one marked in Fig. 7 but appear to be round. A model of the hole marked in Fig. 8(a) is displayed in Fig. 9(b). In this case also surfaces with (111) type orientations show up on the sidewalls. Additional irradiation with the same parameters as in Fig. 8(a) leads to Fig. 8(b). Here the clusters have drilled holes through the whole NiAl wedge. The mechanism is not understood yet. One point to note is that the electron density in platinum is higher than in Ni or Al so that the interaction with the electron beam will be stronger which means that the temperature of the Pt clusters will be higher than that of the NiAl substrate. Thus it is possible that the holes are formed by melting of the substrate below the clusters by the hot clusters. Of course also other physical or chemical interactions are conceivable.

Theoretical considerations for the heating of small clusters by electron beams may be found in Ref. 28. Using the formalism given in this publication we have estimated the current density at which a cluster with a volume of 1.1 nm^3 should melt. The cluster size has been taken from Fig. 6(a) (mean value) ignoring coalescence of clusters as it takes place during heating up. At an energy of 200 keV heating occurs predominantly via ionization processes in the clusters and radiation losses may be ignored.[29] The power density induced by the electron beam depends on the electron density within the clusters (for details see Refs. 28 and 29) which we have corrected for the modified atomic spacing observed for Pt clusters on Al_2O_3/NiAl(110).[4] The current density needed for melting depends strongly on the cluster shape since for flat clusters the heat transfer into the substrate is more efficient than for tall ones. According to our estimate calculations the clusters should melt at current densities between 10^2 and 10^3 A/cm^2 which fits well to the experimental results presented in this article.

It has been shown previously that platinum clusters diffuse through the oxide film into the NiAl substrate at $T \approx 700$ K.[4,7] Such an effect could not be observed in the current study. A possible explanation is that the clusters have destroyed the oxide film below thereby producing a diffusion barrier consisting of the remnants of the oxide film. It could also be the case that the span of time during which the cluster had a temperature appropriate for diffusion through the oxide was too short.

Some type of summary of the present study is displayed in Fig. 10. This figure visualizes the behavior of platinum clusters on Al_2O_3/NiAl(110) as a function of the current density and the irradiation time. It should be viewed as a rough estimate based on the limited set of available data.

IV. SUMMARY AND CONCLUSIONS

For Pt clusters on γ-Al_2O_3(111)/NiAl(110) the influence of irradiation with 200 keV electrons was studied. From the data an approximate current density versus irradiation time phase diagram could be derived which may be summarized as follows: at current densities below about $j=1$ A/cm^2 no modification of the system occurs. Higher current densities induce motion and coalescence and at $j=50$ A/cm^2 decoration of steps takes place. Increasing the current densities to values of $j=150$ A/cm^2 and above leads to the formation of holes in the NiAl substrate with a depth of several 100 Å and edge lengths of some 10 Å.

The change of cluster morphology due to motion and coalescence for current densities between $j=15$ and 80 A/cm^2 was studied in detail. In this range of current densities the irradiation leads to an increase of the mean cluster size and to a reduction of the number of clusters. This effect gets more pronounced with increasing current density. The results open up the possibility to change the cluster size distribution on the surface by electron irradiation in a controlled way. Principally similar effects have to be expected for irradiation with laser beams.

At very high current densities ($j=150$ A/cm^2 and above) holes are burned into the substrate. This may be exploited to produce nanoholes with sizes in the range of some 10 Å which could be used for the production of very small apertures.

ACKNOWLEDGMENTS

The authors thank the Ministerium für Wissenschaft und Forschung des Landes Nordrhein-Westfalen (Referat IV A5, D. Dzwonnek) and the Deutsche Forschungsgemeinschaft for financial support of our work which was partly carried out within the framework of the ''Forschergruppe Modellkat.''

[1]A. K. Datye and D. J. Smith, Catal. Lett. **34**, 129 (1992).
[2]H. Poppa, Catal. Lett. **34**, 129 (1993).
[3]L. D. Marks, Rep. Prog. Phys. **57**, 603 (1994).
[4]M. Klimenkov, S. Nepijko, H. Kuhlenbeck, M. Böumer, R. Schlögl, and H.-J. Freund, Surf. Sci. **391**, 27 (1997).
[5]J. Libuda, M. Bäumer, and H.-J. Freund, J. Vac. Sci. Technol. A **12**, 1 (1994).
[6]Th. Bertrams, F. Winkelmann, Th. Uttich, H.-J. Freund, and H. Neddermeyer, Surf. Sci. **331–333**, 1515 (1995).
[7]M. Bäumer, J. Libuda, H.-J. Freund, G. Graw, Th. Bertrams, and H. Neddermeyer, Ber. Bunsenges. Phys. Chem. **99**, 1181 (1995).
[8]M. Bäumer, J. Libuda, and H.-J. Freund, *Metal Deposits on Thin Well Ordered Oxide Films: Morphology, Adsorption and Reactivity*, in Nato Advanced Study Institute, NATO ASI Series E, edited by R. M. Lambert and G. Pacchioni (Kluwer, Dordrecht, The Netherlands, 1997), Vol. 331, p. 61.
[9]A. Sandell, J. Libuda, P. Brühwiler, S. Andersson, M. Bäumer, A. Maxwell, N. Mårtensson, and H.-J. Freund, J. Vac. Sci. Technol. A **14**, 1546 (1996).
[10]A. Sandell, J. Libuda, P. A. Brühwiler, S. Andersson, M. Bäumer, A. Maxwell, N. Mårtensson, and H.-J. Freund, J. Electron Spectrosc. Relat. Phenom. **76**, 301 (1995).
[11]K. Wolter, O. Seiferth, J. Libuda, H. Kuhlenbeck, M. Bäumer, and H.-J. Freund, Surf. Sci. (accepted for publication).
[12]T. Kizuka and N. Tanaka, Philos. Mag. Lett. **76**, 289 (1997).
[13]T. J. Bullough, Philos. Mag. A **75**, 69 (1997).
[14]P. Williams, Appl. Phys. Lett. **50**, 1760 (1987).
[15]M. Mitome, Y. Tanishiro, and K. Takayanagi, Z. Phys. D **12**, 45 (1989).
[16]S. Iijima and T. Ichihashi, Phys. Rev. Lett. **56**, 616 (1986).
[17]A. Howie, Nature (London) **320**, 684 (1986).
[18]N. Doraiswamy and L. D. Marks, Surf. Sci. **348**, L67 (1996).
[19]P. M. Ajayan and L. D. Marks, Phys. Rev. Lett. **63**, 279 (1989).
[20]P. M. Ajayan and L. D. Marks, Phys. Rev. Lett. **60**, 585 (1988).
[21]R. M. Jaeger, H. Kuhlenbeck, H.-J. Freund, M. Wuttig, W. Hoffmann, R. Franchy, and H. Ibach, Surf. Sci. **259**, 235 (1991).
[22]J. Libuda, F. Winkelmann, M. Bäumer, H.-J. Freund, Th. Bertrams, H. Neddermeyer, and K. Müller, Surf. Sci. **318**, 112 (1961).
[23]M. Klimenkov, S. Nepijko, H. Kuhlenbeck, and H.-J. Freund, Surf. Sci. **385**, 66 (1997).
[24]N. J. Long, R. F. Marzke, M. McKelvy, and W. S. Glaunsinger, Ultramicroscopy **20**, 15 (1986).
[25]S. Wohlrab, F. Winkelmann, H. Kuhlenbeck, and H.-J. Freund, *Adsorption on Epitaxial Oxide Systems as Model Systems for Heterogeneous Catalysis*, in Surface Science: Principles and Current Applications, edited by R. J. McDonald, E. C. Taglauer, and K. Wandelt (Springer, Berlin, Germany, 1996), p. 193.
[26]L. Reimer, *Transmission Electron Microscopy: Physics of Image Formation and Microanalysis*, Springer Series in Optical Sciences (Springer, Berlin, 1997), p. 287ff.
[27]L. Reimer, *Transmission Electron Microscopy: Physics of Image Formation and Microanalysis*, Springer Series in Optical Sciences (Springer, Berlin, 1997), p 293.
[28]V. G. Gryaznov, A. M. Kaprelov, and A. Y. Belov, Philos. Mag. Lett. **63**, 275 (1991).
[29]L. Reimer, *Transmission Electron Microscopy: Physics of Image Formation and Microanalysis*, Springer Series in Optical Sciences (Springer, Berlin, 1997), p. 563ff.